Development 138, 2467-2476 (2011) doi:10.1242/dev.054106

Restoring eye size in *Astyanax mexicanus* blind cavefish embryos through modulation of the *Shh* and *Fgf8* forebrain organising centres

Karen Pottin, Hélène Hinaux and Sylvie Rétaux*

SUMMARY

The cavefish morph of the Mexican tetra (*Astyanax mexicanus*) is blind at adult stage, although an eye that includes a retina and a lens develops during embryogenesis. There are, however, two major defects in cavefish eye development. One is lens apoptosis, a phenomenon that is indirectly linked to the expansion of ventral midline sonic hedgehog (*Shh*) expression during gastrulation and that induces eye degeneration. The other is the lack of the ventral quadrant of the retina. Here, we show that such ventralisation is not extended to the entire forebrain because fibroblast growth factor 8 (*Fgf8*), which is expressed in the forebrain rostral signalling centre, is activated 2 hours earlier in cavefish embryos than in their surface fish counterparts, in response to stronger Shh signalling in cavefish. We also show that neural plate patterning and morphogenesis are modified in cavefish, as assessed by *Lhx2* and *Lhx9* expression. Inhibition of Fgf receptor signalling in cavefish with SU5402 during gastrulation/early neurulation mimics the typical surface fish phenotype for both *Shh* and *Lhx2/9* gene expression. Fate-mapping experiments show that posterior medial cells of the anterior neural plate, which lack *Lhx2* expression in cavefish, contribute to the ventral quadrant of the retina in surface fish, whereas they contribute to the hypothalamus in cavefish. Furthermore, when *Lhx2* expression is rescued in cavefish after SU5402 treatment, the ventral quadrant of the retina is also rescued. We propose that increased Shh signalling in cavefish causes earlier *Fgf8* expression, a crucial heterochrony that is responsible for *Lhx2* expression and retina morphogenesis defect.

KEY WORDS: Lhx2, Heterochrony, Neural plate

INTRODUCTION

The teleost fish *Astyanax mexicanus* exists in two forms: a surface-dwelling river morph and a cave-living blind morph. The two forms of this single species split from a common ancestor about 1 million years ago, a relative short period of time during which the cave animals have evolved both regressive and constructive features (Jeffery, 2001). The loss of eyes and pigmentation, and the increase in feeding apparatus (jaws, teeth, taste-buds) (Varatharasan et al., 2009; Yamamoto et al., 2009) and body fat content (Rose and Mitchell, 1982; Salin et al., 2010) are distinctive features of cavefish when compared with their surface counterparts. *Astyanax* embryos are therefore excellent models with which to analyse the molecular and cellular developmental mechanisms of morphological evolution (Jeffery, 2008; Jeffery, 2009; Rétaux et al., 2008).

The anterior expression domain of the morphogen sonic hedgehog (*Shh*) at the embryonic ventral midline is expanded throughout cavefish forebrain development (Menuet et al., 2007; Yamamoto et al., 2004). The secondary loss of eyes is the most spectacular indirect consequence of this increased Shh signalling (Yamamoto et al., 2004). However, expanded *Shh* also causes significant and specific modifications in the ventral telencephalon and hypothalamus. In fact, Shh-dependent variations in proliferative activity and in expression of *Nkx* and LIM-homeodomain transcription factors induce variations in specification and migrations of specific neuronal populations (Menuet et al., 2007). Besides these specific changes, the global early patterning of the forebrain, including the retina, is normal in cavefish. Indeed, the cavefish eyes undergo normal morphogenesis, growth and patterning during the first 24 hours of development, except for a slightly smaller retina size and a reduced or absent ventral quadrant of the retina, a hallmark of the cavefish embryonic eye (Alunni et al., 2007; Yamamoto and Jeffery, 2000; Yamamoto and Jeffery, 2002). The degeneration and loss of eyes in cavefish occur later and progressively in the following days and weeks (Alunni et al., 2007; Jeffery, 2001; Jeffery, 2005; Wilkens, 2007), and are triggered by lens apoptosis which starts after the first day of development (Strickler et al., 2007; Yamamoto and Jeffery, 2000). Thus, the marked increase in midline *Shh* expression in cavefish embryos does not have the deleterious consequences one might expect for such a powerful morphogen (for a review, see Monuki, 2007). This is strongly suggestive of compensation or balancing mechanism(s) that would 'protect' the cavefish forebrain from being totally disorganised by *Shh* expansion.

In all vertebrates, including fish, the anterior neural plate gives rise to the forebrain, including the telencephalon and the diencephalon, from which the optic vesicles and the hypothalamus develop. The growth, the morphogenesis and the patterning of the anterior neural plate are controlled by the concerted action of molecules secreted from signalling centres (also called secondary organisers) that diffuse through the neuroepithelium and impose a field of organisation (for a review, see Vieira et al., 2010). These signalling centres are mostly located along the embryonic midline and secrete morphogens such as Shh (Echelard et al., 1993), Wnt (wingless-Int) (Lee and Jessell, 1999; Muroyama et al., 2002) and

Equipe Développement Evolution du Cerveau Antérieur, UPR3294 NeD, CNRS, Institut Alfred Fessard, 91198 Gif-sur-Yvette, France.

*Author for correspondence (retaux@inaf.cnrs-gif.fr)

Accepted 29 March 2011

Sfrp (secreted frizzled related protein) (Houart et al., 2002), Bmp (bone morphogenetic protein) (Liem et al., 1997) or Fgf (fibroblast growth factor) (Shimamura and Rubenstein, 1997) molecules. Thus, the ventral signalling centre (notochord, and later floor and basal plate of the neural tube) secretes Shh, which induces ventral forebrain structures, whereas the rostral signalling centre (anterior neural ridge and telencephalon) secretes several Fgfs, including Fgf8 (Miyake et al., 2005), which is crucial for olfactory bulb growth and pallial patterning (Fukuchi-Shimogori and Grove, 2001; Shimogori et al., 2004; Storm et al., 2006).

A few studies have addressed the cross-regulatory interactions between signalling centres that shape the forebrain (Crossley et al., 2001; Hayhurst et al., 2008; Ohkubo et al., 2002; Okada et al., 2008; Shanmugalingam et al., 2000; Storm et al., 2006), but little is known about their relative influence, how they can modulate forebrain morphogenesis, or to what extent their tight regulation in time is crucial. Moreover, most studies are based on gain- or loss-of-function approaches in laboratory animals, which usually lead to lethal conditions. Here, we have used the *Astyanax* cavefish embryo as a natural mutant to study secondary organiser's interactions in time and space, as well as their developmental outcome in a physiological and adaptive context. We show that cavefish embryos express *Fgf8* 2 hours earlier than surface fish embryos, a heterochrony that has essential implications for anterior neural plate patterning at early stage and that is also responsible for retina morphogenesis defect at later stage. By interfering pharmacologically with this *Fgf8* heterochrony, we were able to rescue the ventral quadrant of the cavefish retina, i.e. to rescue the neural component of the eye defect in cavefish.

MATERIALS AND METHODS

Fish samples

Laboratory stocks of *A. mexicanus* surface fish and cavefish (Pachòn population) were obtained in 2004 from the Jeffery laboratory at the University of Maryland, College Park, MD. Fish are maintained at 23-26°C on a 12:12 hours light:dark cycle. Embryos were collected after spawning and fixed at various stages in 4% paraformaldehyde (PFA). After progressive dehydration in methanol, they were stored at –20°C. *A. mexicanus* development is highly similar to zebrafish in the first 20 hours post-fertilisation (hpf) and, importantly, there is no difference in early developmental timing between the cave and surface forms (H.H, K.P, H. Chaloub, S. Père, Y. Elipot, L. Legendre and S.R., unpublished; see Fig. S3 in the supplementary material).

cDNA cloning

Total RNA from cavefish embryo at 20 hpf was reverse transcribed with random primers using AMV reverse transcriptase (Promega). Partial cDNA sequence for *Fgf3* (341 bp, GenBank HQ667934) was amplified by PCR using degenerated primers designed after alignments of several teleost sequences (sequences available on request). PCR products were subcloned in TOPO-PCR II vector (Invitrogen) and sequenced. *Shh* (AY661431), *Nkx2.1a* (AY661435) and *Bmp4* (DQ915173) cDNA were previously isolated by the Jeffery and Stock laboratories, and *Fgf8* (DQ822511), *Lhx2* (EF175737) and *Lhx9* (EF175738) cDNAs were previously cloned by our group (Alunni et al., 2007).

Whole-mount in situ hybridisation

cDNAs were amplified by PCR, and digoxygenin- or fluorescein-labelled riboprobes were synthesised from PCR templates. A protocol for automated whole-mount in situ hybridisation (Intavis) was performed (Deyts et al., 2005).

For fluorescent in situ hybridisation, Cy3- and FITC-tyramides were prepared as described (Zhoua and Vize, 2004). Embryos were incubated with antibody anti-FITC-POD (Roche, 1/250), washed in PBS/Tween 0.1% (PBST) and incubated for 20 minutes at room temperature with FITC-tyramide at 1/100. Tyramides were activated by H_2O_2 (Sigma, 0.001%) for 30 minuets and washed again in PBST. The first peroxydase conjugate was inactivated by incubation in 2% H_2O_2 for 1 hour. Embryos were washed in PBST and incubated with the second antibody (anti-digoxygenin-POD, Roche, 1/250). The same protocol was applied for the Cy3-tyramide revelation.

Quantitative real time RT-PCR

Total RNA was extracted from head or tail at 10 hpf (0 somite) or 14 hpf (10 somites) of cavefish or surface fish embryos using RNA TRIzol. cDNAs were synthesised using SuperScript II (Invitrogen) and PCR was performed using dsDNA dye SYBR Green I (Roche Diagnostics). Primer pairs for *Fgf8* (sense, 5′-GCAGGCTAATACGGACC-3′ and antisense, 5′-ACTGCCGAATGTGTCT-3′) and control α-actin (sense, 5′-CATTA-CCAACTGGGACG-3′, and antisense, 5′-TCTTCTCACGGTTAGCC-3′) were used to detect target gene transcripts. SYBR Green analysis was performed on a Lightcycler (Roche Diagnostics). All samples were analyzed in duplicate in three independent experiments, and the amount of mRNA detected was normalised to control α-actin mRNA values. We used normalised data to quantify the relative levels of *Fgf8* mRNA according to cycling threshold analysis (ΔCt).

SU5402 and cyclopamine treatments

For incubation with the FGFR inhibitor SU5402 (Calbiochem), embryos were dechorionated manually and allowed to develop in embryo medium containing Methylene Blue (EMM) in petri dishes coated with a layer of 1% agarose. Upon reaching the desired stage, they were incubated in SU5402 diluted in EMM from a 3 mM stock solution in DMSO. Control embryos had an equivalent volume of DMSO added to the EMM. Following incubation, embryos were washed gently in several changes of EMM and fixed immediately (at six somites), or allowed to develop until 27 hpf.

For incubation with cyclopamine (Toronto Research Chemicals), the same protocol was used. Control embryos were exposed to 0.1% ethanol, as the cyclopamine stock solution was diluted in 100% ethanol.

Quantification of expression pattern modification was performed manually on in toto pictures of embryos at 12 hpf (six somites) photographed in the same orientation using agarose wells. For the measurement of the CF ventral quadrant and lens, ImageJ was used. All the data come from at least three independent experiments and statistical comparisons were performed using a Student's *t* test.

Dextran iontophoresis

The method was adapted from The Zebrafish book (Westerfield, 2000). Briefly, dextran tetramethyl-rhodamine (D3308, Molecular Probes) in KCl 0.1 M was injected into the neural plate of 10 hpf embryos embedded in 3% methyl cellulose under the control of a fluorescence stereomicroscope (200×, Leica). Embryos were individually photographed 1 hour after injection. Embryos were transferred into wells coated with 1% agarose and kept in 1.5 ml EMM at 23°C. The next day, embryos were anesthetised in tricaine methane sulphate (MS222, Sigma, 0.2 mg/ml) and their eyes and brain were photographed using an Apotome microscope (Zeiss). For the fate map analysis, the neural plate of each embryo was outlined using the bright-field picture (Fig. 5A,H). Fluorescent pictures were superimposed and injection domains were reported on the neural plate drawing (Fig. 5A′,H′). According to the progeny observed at 27 hpf, a colour was attributed to the injection domain. Finally, all the individual neural plate drawings were superimposed and a fate map was obtained.

RESULTS

Fgf8 is turned on 2 hours earlier in the cavefish telencephalon

In cavefish (CF), the *Shh* ventral midline expression domain is expanded laterally and anteriorly, throughout gastrulation, neurulation and later on, when compared with surface fish (SF) (Fig. 1A-C′; see Fig. S1A,A′ in the supplementary material) (Yamamoto et al., 2004). Such expansion concerns various tissues as development proceeds. At the end of gastrulation and early neural plate stage (i.e. before

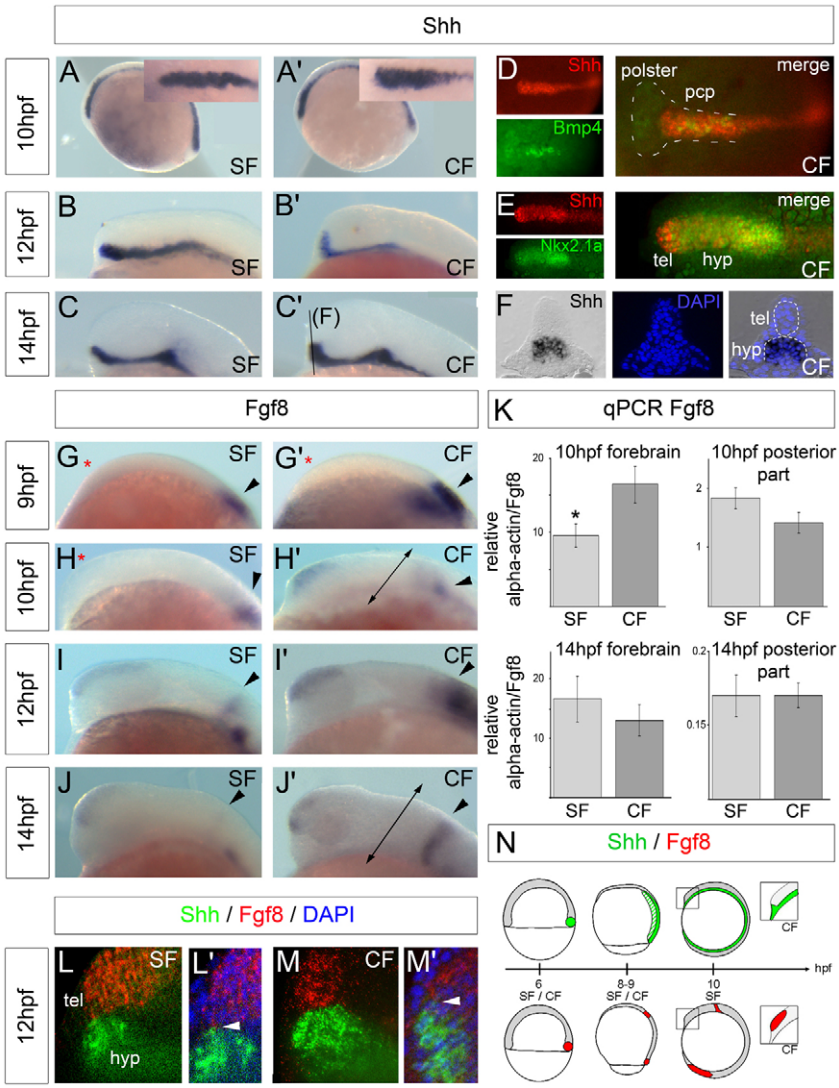

Fig. 1. *Shh* and *Fgf8* expression patterns in SF and CF. Anterior is leftwards and dorsal is upwards. (**A-C′**) *Shh* expression at 10 hpf (A,A′), 12 hpf (B,B′) and 14 hpf (C,C′) on lateral views. *Shh* is expanded anteriorly and laterally (insets in A,A′) in CF. (**D**) Double fluorescence in situ hybridisation for *Shh* (red) and *Bmp4* (green, a prechordal and polster marker) showing that *Shh* is enlarged in the prechordal plate (PcP) of a 10 hpf CF embryo. (**E**) Double fluorescence in situ hybridisation for *Shh* (red) and *Nkx2.1a* (green, a hypothalamic marker) showing that *Shh* is enlarged in the ventral neural tube, including the hypothalamus (hyp) and the anterior-most telencephalon (tel) of a 12 hpf CF embryo. (**F**) Second rostralmost frontal section through a 14 hpf CF showing that *Shh* is enlarged in the hypothalamus. DAPI counterstaining of nuclei is in blue. See Fig. S2 in the supplementary material for the complete anteroposterior series of sections. (**G-J′**) *Fgf8* expression at 9 hpf, 10 hpf, 12 hpf and 14 hpf. *Fgf8* is expressed in the telencephalon from 10 hpf in CF and from 12 hpf in SF. Black arrowheads indicate the MHB, red asterisks indicate absence of *Fgf8* expression and double-headed arrows indicate the level where the 'forebrain' (=telencephalon) and 'posterior part' (=mhb+tailbud) samples were cut for subsequent qPCR analysis. (**K**) Histograms of qRT-PCR results showing increased levels of *Fgf8* mRNA relative to α-actin mRNA in the CF head at 10 hpf. **P*<0.05 in one-way ANOVA comparing SF and CF mRNA levels (*n*=3). (**L-M′**) Double fluorescence in situ hybridisation for *Shh* (green) and *Fgf8* (red) transcripts. The two transcripts are never expressed in a same cell. A white arrowhead indicates the boundary between the two domains. (**N**) Scheme of *Shh* (green) and *Fgf8* (red) expression patterns during gastrulation and at the beginning of neurulation in *Astyanax*. At 10 hpf in CF (insets), *Shh* is expanded anteriorly and *Fgf8* is already expressed in the telencephalon.

neurulation, which starts at 10 hpf in *Astyanax;* see Fig. S1B,B′ in the supplementary material), *Shh* expansion concerns the axial ventral midline represented at its rostral tip by the *Bmp4*-positive prechordal plate (PcP) (Fig. 1D). After neurulation, at 12 hpf (5-6 somites), *Shh* expansion concerns the medial/ventral part of the neural tube, which corresponds to the *Nkx2.1a*-positive presumptive hypothalamus, and also very transiently to the ventralmost telencephalon (Fig. 1E). Two hours later, at 14 hpf (11-12 somites), *Shh* expression is still expanded in the hypothalamus (Fig. 1F and see Fig. S2 in the supplementary material).

We hypothesised that other signalling molecules may be modified at the CF anterior neural plate. Among those tested and compared in CF and SF embryos between 10 hpf and 16 hpf, *Fgf8* expression showed a difference. In fact, *Fgf8* was detectable by in situ hybridisation in the CF telencephalon as early as 10 hpf, whereas it was apparent only at 12 hpf in SF (Fig. 1G-J′). Of note, earlier expression domains of *Fgf8* in the shield at 6-7 hpf and in the tailbud and the presumptive mid-hindbrain junction (mhb) at 8-9 hpf was identical in the two populations (see Fig. S1C-D′ in the supplementary material), and expression was indistinguishable again at 14 hpf (Fig. 1J-J′). Importantly, the timing of neurulation which starts between 9.6 hpf and 10 hpf, and is completed by 12 hpf in *Astyanax*, is totally synchronous between CF and SF embryos (see Fig. S3 in the supplementary material), ruling out the possibility that *Fgf8* expression heterochrony could be due to differences in developmental timing of the morphogenesis between the two populations of embryos.

To confirm these qualitative observations in a quantitative manner, we performed real-time quantitative RT-PCR (Fig. 1K). At 10 hpf, *Fgf8* transcripts were 42% more abundant in the forebrain of CF embryos when compared with their SF counterparts, whereas the posterior part of SF and CF embryos (including the mhb and tailbud expression domains) contained similar *Fgf8* transcript levels. No difference was observed in the 14 hpf samples, confirming the in situ hybridisation data. As several Fgfs, including Fgf3, are implicated in early telencephalic Fgf signalling (Walshe and Mason, 2003), we also compared *Fgf3* expression in CF versus SF. The two types of embryos showed identical *Fgf3* patterns at crucial time points between 9.5 hpf and 12 hpf (and later, not shown), including in the telencephalon, mhb and rhombomere 4 (see Fig. S1F-G′ in the supplementary material). In summary, these comparative expression data show a heterotopy of *Shh* expression in the PcP and the hypothalamus and a heterochrony of *Fgf8* expression in the telencephalon at stages between 10 and 12 hpf, i.e. when these two signalling systems organise the anterior neural plate and future forebrain.

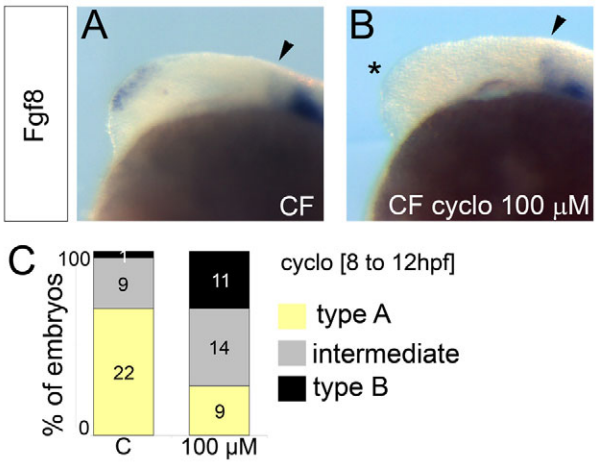

Fig. 2. Cyclopamine treatment affects *Fgf8* expression in the telencephalon but not the mhb. (**A**,**B**) Anterior is leftwards and dorsal is upwards. *Fgf8* expression in a 12 hpf control CF (A) and a CF incubated in 100 μM cyclopamine from 8 to 12 hpf (B). The arrowheads indicate the MHB. Asterisk indicates the absence of *Fgf8* expression after cyclopamine treatment. (**C**) Quantification of cyclopamine effect. The *y*-axis indicates the percentage of embryos with a given phenotype and the number of scored embryos is indicated in columns. Type A is the wild-type CF phenotype (yellow, shown in A). Type B showed no *Fgf8* expression in the dorsal forebrain (black, shown in B). Intermediate embryos (grey) showed diminished/faint *Fgf8* expression.

We next examined whether the *Shh-Fgf8* spatial relationship is modified between the two populations. Double fluorescence in situ hybridisation revealed that in both CF and SF embryos, the two expression domains – the *Fgf8*-positive telencephalon (alar plate) and the *Shh*-positive hypothalamus (basal plate) – are strictly adjacent and never overlap, with their boundary being shifted dorsally in CF (Fig. 1L-M′). Neighbouring cells express one or the other factor but never both (Fig. 1L′,M′, arrowheads). Thus, the Shh and the Fgf8 signalling centres progress from the shield towards the anterior pole of the embryo as gastrulation and axis formation proceed (Fig. 1N). At 10 hpf, the future forebrain of CF embryos expresses significantly more transcripts for the two signalling molecules than its SF counterpart. The *Fgf8* heterochrony therefore probably explains why the CF forebrain is not ventralised, as one might expect from its *Shh* pattern.

Fgf8 heterochrony in CF is due to increased Shh signalling

We next sought to determine the origin of the *Fgf8* heterochrony in CF. We analysed the possibility that *Fgf8* is expressed earlier because *Shh* domain is expanded early on (Fig. 1A′; see Fig. S1A′,B′ in the supplementary material). We treated CF embryos with cyclopamine, an inhibitor of Shh signalling (Chen et al., 2002; Incardona et al., 1998). Embryos treated with 100 μM cyclopamine between 80% epiboly (8 hpf) and six somites (12 hpf) and grown to 27 hpf had their eyes localised more anteriorly than normal (mild pre-cyclopia phenotype), confirming the efficiency of the drug. CF embryos treated in these conditions had a normal mhb *Fgf8* pattern but showed reduced or no *Fgf8* telencephalic expression at 12 hpf (Fig. 2A-C), demonstrating a role for Shh in *Fgf8* induction, and suggesting that high Shh signalling in CF is responsible for the earlier onset of *Fgf8* expression.

Interfering with Fgf signalling in CF mimics SF phenotype

To test whether the *Fgf8* heterochrony compensates for enlarged *Shh* expression, we treated CF embryos with SU5402, an inhibitor of Fgf receptor signalling (Mohammadi et al., 1997) that is effective on *Astyanax* embryos (Gibert et al., 2010). The treatment was performed using two time windows, either from 50% epiboly (6 hpf) or from 80% epiboly (8 hpf) to six somites (12 hpf). CF embryos incubated in SU5402 displayed a *Shh* expression pattern that mimicked the typical SF pattern (Fig. 3A-D). For quantification, embryos were scored according to the following criteria: (1) type A embryos, *Shh* expanded anteriorly as in a typical CF embryo; (2) type B embryos, *Shh* expression less expanded rostrally; (3) type C embryos, *Shh* expression like in a typical SF embryo. Examples of type A, type B and type C embryos are shown in Fig. 3A,B and C, respectively. Using this scoring method, the effect of SU5402 was found to be dose-dependent between 0.75 and 5 μM of the inhibitor and was more pronounced when the large window of treatment was used (Fig. 3E-F). This indicated that Fgf signalling is required for the stimulation and/or the maintenance of *Shh* expansion in CF embryos.

We also examined whether *Fgf8* expression is dependent upon FgfR signalling. SU5402 treatment on CF resulted in lateral and ventral expansion of the telencephalic *Fgf8* pattern (Fig. 3G-J). Again, this effect was dose dependent when assessed using the same type of scoring method as above (Fig. 3K). The *Fgf8* ventral expansion is correlated to the Shh posterior shift in the same condition of SU5402 treatment observed above, and the *Fgf8* lateral expansion suggests an FgfR-dependent negative feedback loop on *Fgf8* expression. In summary, pharmacological treatments of CF embryos allow the unmasking of several interactions between Shh and Fgf8 signalling centres, including their reciprocal stimulation and an FgfR-dependent negative-feedback loop on *Fgf8* expression (Fig. 3L). Of note, the direct or indirect nature of these interactions is unknown.

Fgf8 heterochrony influences anterior neural plate development

We next asked to what extent the spatiotemporally modified signalling centres in CF affect anterior neural plate and early forebrain patterning and morphogenesis. To address this issue, we first used two LIM-homeodomain factors involved in eye and forebrain development, *Lhx2* and *Lhx9*, as regionalisation markers (Atkinson-Leadbeater et al., 2009; Porter et al., 1997; Tetreault et al., 2009; Yun et al., 2009; Zuber et al., 2003). Both factors showed significantly different expression patterns in CF and SF at 10 hpf (neural plate stage, Fig. 4A,A′, summarised on Fig. 4F,F′) and 12 hpf (closed neural plate, Fig. 4B-C′,D-E′). In SF, the expression of the two genes covered the entire presumptive forebrain area, whereas in CF *Lhx2* expression was absent from its medial posterior part (asterisks in Fig. 4) and *Lhx9* expression was absent from its medial anterior part (arrowheads in Fig. 4). Of note, the differential patterns of *Lhx2* and *Lhx9* appear spatially correlated to those of *Shh* and *Fgf8* (Fig. 4A,A′ for *Lhx2*/*Shh*).

Because SU5402-treated CF embryos display a SF-like *Shh* expression pattern (Fig. 3), we next analysed *Lhx2* and *Lhx9* expression patterns at 12 hpf after FgfR signalling inhibition. This treatment on CF mimicked the SF phenotype and restored SF-like *Lhx2* and *Lhx9* patterns at the posterior and anterior midline, respectively (Fig. 4G-K). The effects were dose

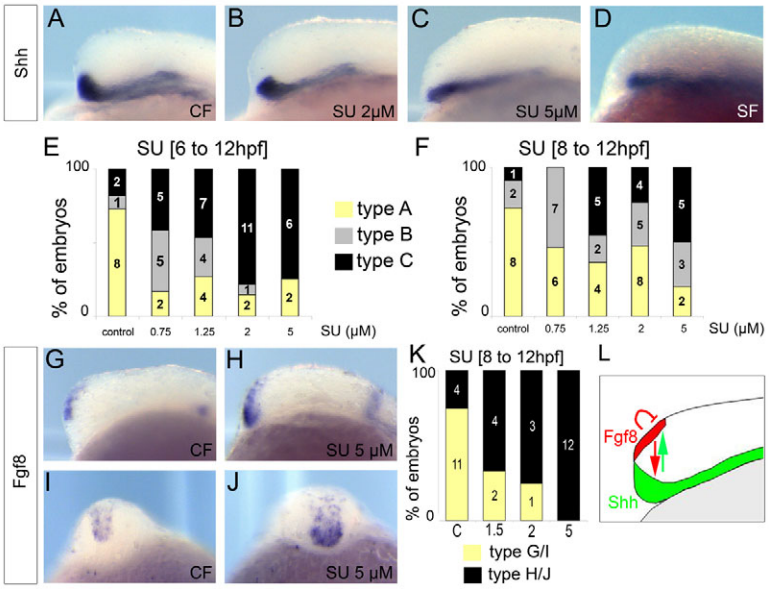

Fig. 3. SU5402 treatment affects *Shh* and *Fgf8* expression. (**A-D**) Anterior is leftwards and dorsal is upwards.12 hpf *Shh* expression in control CF (A), in CF incubated with increasing concentrations of SU5402 (B,C) or in SF (D). Note the progressive 'retraction' of *Shh* expression with 2 and 5 µM SU5402, mimicking the SF typical *Shh* pattern. (**E**,**F**) Quantification of SU5402 effect on *Shh* expression after longer (from 6 hpf to 12 hpf, E) or shorter (from 8 hpf to 12 hpf, F) treatment on CF. The *y*-axis indicates the percentage of embryos with a given phenotype and the number of scored embryos is indicated in columns. Type A is the wild-type CF phenotype (yellow, shown in A). Type C showed strongly retracted, SF-like, *Shh* expression at the PcP (black, shown in C/D). Type B showed intermediate pattern (grey, shown in B). Note that for both windows of treatment, the effects are dose dependent between 0.75 and 5 µM of SU5402 compound. (**G-J**) *Fgf8* expression in a 12hpf control CF (G, lateral view; I, frontal view) and a CF incubated in 5 µM SU5402 from 8 to 12 hpf (H, lateral view; J, frontal view). (**K**) Quantification of effect of SU5402 on *Fgf8* expression after an 8 hpf to 12 hpf treatment on CF. Type G/I (yellow) is the wild-type CF phenotype. Type H/J (black) is the affected phenotype, showing lateral enlargement and anterior expansion of the *Fgf8* domain. (**L**) Summary drawing of the regulatory interactions between Fgf8 and Shh signalling centres unmasked by cyclopamine and SU5402 treatments.

dependent, in the same range of concentrations as those that affect *Shh* expression (Fig. 4I,K). Thus, the CF anterior neural plate appears differentially organised, owing to its special signalling centres.

Precocious inhibition of Fgf signalling affects later retina morphogenesis

As *Lhx2* is a major factor for eye field specification and morphogenesis (Porter et al., 1997; Tetreault et al., 2009; Yun et al., 2009; Zuber et al., 2003), we next hypothesised that its modified pattern in CF may indicate different fates and/or movements of the posterior medial cells, and may be responsible for the absence of the ventral quadrant (vq) of the retina in CF embryos.

First, we determined the fate of the cells located in the medial posterior part of the presumptive forebrain, which express *Lhx2* in SF but not in CF. Dextran iontophoresis was applied in the anterior neural plate, including in this zone on 10 hpf embryos (Fig. 5A-A″,H-H″). The progeny of labelled cells was analysed 17 hours later (i.e. at 27 hpf) (Fig. 5B-E,I-J″).

In SF, the vast majority of injections led to the observation of labelled cells located in the retina, including the vq, and in the hypothalamus, at 27 hpf (31 out of 34 successfully injected embryos) (Fig. 5F,G). When injections targeted cells located in the posterior and medial *Lhx2*-positive SF neural plate, the labelled progeny contributed to the vq (*n*=10, pink) or to both the vq and the dorsal retina (*n*=5, black), or else to both the vq and the hypothalamus (*n*=3, dark blue). When injections targeted cells located either more laterally or more anteriorly in the neural plate, the labelled progeny contributed to the dorsal retina (*n*=10, green) but neither to the vq nor to the hypothalamus (Fig. 5G). These data demonstrate that in SF, some of the cells located in the medial posterior part of the *Lhx2*-positive domain at neural plate stage give rise to the vq of the retina (Fig. 5F,G).

In CF, the deduced fate map was different (Fig. 5K). The general trend from 27 successfully injected CF embryos was an absence of cells fated to give rise to the vq (except for one cell in a CF specimen naturally possessing a small vq), and an enlargement of the presumptive territory for the basal diencephalon/hypothalamus. In fact, when injections targeted cells located in the posterior and medial *Lhx2*-negative CF neural plate, their major contribution was the hypothalamus (*n*=7/7, light blue) together with the dorsal retina (*n*=4/7, green). When injections were more lateral or anterior in the neural plate, their fate was the dorsal retina as in SF, but a large contribution to the hypothalamus was also found (*n*=9/15, light blue). In summary, these comparative fate maps show that SF and CF posterior medial forebrain neural plate give rise to distinct structures, suggesting a trade-off between ventral retina- and hypothalamic-fated territories in CF, and confirming major differences in patterning and cell movements in CF and SF at these stages.

Finally, we treated CF embryos with SU5402 between 8 and 12 hpf, and let them grow until 27 hpf. In these larvae, the vq was rescued (Fig. 5L,M) and was often indistinguishable from the SF normal eyes (Fig. 5N). Measurements of retina and vq sizes showed that upon SU5402 treatment, the vq contribution to eye size increases by ~50% (Fig. 5O). Conversely, SU5402 caused a

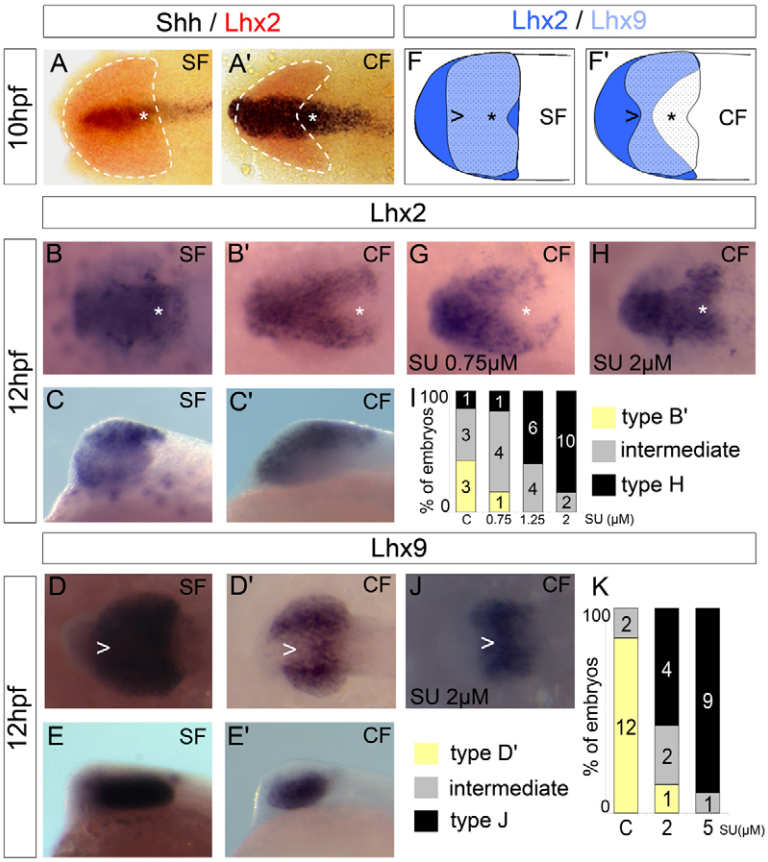

Fig. 4. *Lhx2* and *Lhx9* patterns differ between CF and SF and are affected by SU5402 treatment. Anterior is leftwards and dorsal is upwards. (**A-E′**) Dorsal and lateral views of SF (lA-E) and CF (A′-E′) embryos hybridised with the indicated probes and at the indicated stages. At 10 hpf the expression of *Lhx2* (and *Lhx9*, not shown) on dorsal views appears large, indicating a 'flat' neural plate. At 12 hpf, it appears narrower because neurulation and keel formation is almost finished (see also Fig. S3 in the supplementary material). On dorsal views, the position in the neural plate where *Lhx2* and *Lhx9* expression is observed in SF but not in CF is indicated by symbols (asterisk for Lhx2, arrowheads for Lhx9). (**F**,**F′**) Composite summary of the compared *Lhx2* and *Lhx9* patterns in SF and CF. (**G-I**) Effect of SU5402 treatment on *Lhx2* expression and quantification. The *y*-axis indicates the percentage of embryos with a given phenotype and the number of scored embryos is indicated in columns. Type B′ is the wild-type CF phenotype (yellow, arrow-shaped) *Lhx2* pattern. Type G (grey) and type H (black) showed intermediate and SF-like phenotypes, respectively. (**J**,**K**) Effect of SU5402 treatment on *Lhx9* expression and quantification. Type D′ is the wild-type CF phenotype (yellow, butterfly-shaped) *Lhx9* pattern. Type intermediate (grey) and type J (black) embryos showed intermediate and SF-like phenotypes, respectively.

small but significant reduction of the size of the lens (Fig. 5O), which must probably be attributed to modifications of the placodal field (Toro and Varga, 2007).

DISCUSSION

The eye defect in CF embryos has two components. One is placode related, as the triggering event for eye degeneration is lens apoptosis. The other is neural plate related, as the CF retina is smaller than the SF retina and lacks a normal vq. Here, we provide evidence that the neural plate component of the CF eye defect is driven by modifications not only in space (Shh) but also in time (Fgf8) of the expression of signalling molecules that shape the forebrain at neurula stage. The latter probably also explains why the entire CF forebrain is not ventralised by *Shh* overexpression (Fig. 6).

Cavefish: a natural mutant with which to analyse interactions between signalling centres

Several papers have reported the function of Shh or Fgf8 molecules through analysis of zebrafish or mouse mutants or loss-of-function experiments. Here, we have taken advantage of the two *Astyanax* populations to study and uncover the impact of subtle spatial and temporal modifications of these signalling pathways on forebrain morphogenesis. In this model system, the SF are considered as the 'wild-type' animals, whereas the CF and their expanded embryonic Shh expression domain and blind adult phenotype are viewed as the 'mutants'. The advantage we see in this comparison is that the modifications we uncover in CF embryos are probably adaptive, as genetic analyses have shown that mutations in genes affecting the eye phenotype in CF are driven by natural selection (Protas et al., 2007).

We found a 2 hours difference in the appearance of *Fgf8* transcripts between the two populations. We interpret this finding by proposing that a Shh threshold level is reached earlier in the CF anterior neural plate, as suggested by cyclopamine experiments. Such threshold effects were recently demonstrated for Shh signalling controlling facial morphogenesis (Young et al., 2010). This is also consistent with mammalian data showing a loss of *Fgf8* expression in the anterior neural ridge of *Shh* mouse mutants (Hayhurst et al., 2008; Ohkubo et al., 2002), and with zebrafish data showing that cyclopamine treatment from 5 hpf to 15 hpf decreases telencephalic but not mhb *Fgf8* expression (Miyake et al., 2005). In both fish species and in mammals, Shh therefore appears to stimulate *Fgf8* expression at the rostral telencephalon.

In turn, we show with SU5402 experiments that FgfR signalling allows the maintenance of *Shh* overexpression in the PcP and hypothalamus. We observed subtle but significant differences in the results depending on the time-window used for the SU5402 treatment. More embryos were affected when the drug was applied from 6 to 12 hpf when compared with the 8 to 12 hpf window. This indicates that a stimulation of *Shh* expression through FgfR signalling occurs throughout gastrulation and the beginning of neurulation. Of note, similar interactions were described in the neural plate in other species. For example, a reduction in Fgf8 dose leads to a diminution of *Shh* expression in the mouse subpallium (Storm et al., 2006). In addition, in zebrafish, *Shh* is not expressed in the telencephalon of ace (*Fgf8a*) mutants (Shanmugalingam et al., 2000), and injection of *Fgf8* and *Fgf3* morpholinos decrease hypothalamic *Shh* expression (Walshe and Mason, 2003).

Shh and Fgf8 are powerful morphogens, known to be implicated in the control of cell proliferation. In CF, the *Shh* expression domain is expanded and *Fgf8* is expressed precociously, suggesting

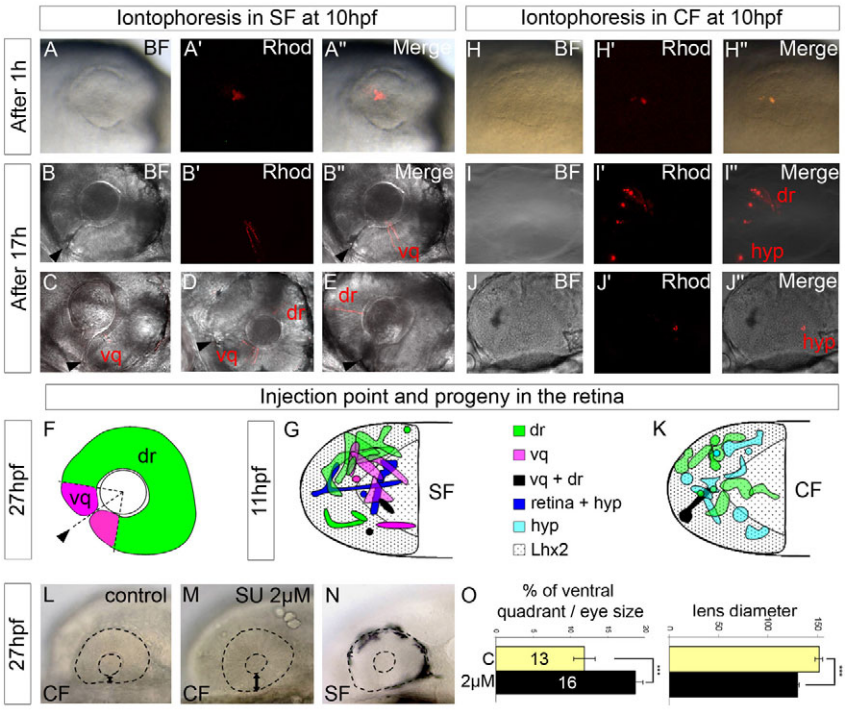

Fig. 5. Comparative fate-mapping of the eye-field in SF and CF, and SU5402-induced rescue of the retina ventral quadrant in CF. Anterior is leftwards and dorsal is upwards. (**A-E**) Rhodamine dextran iontophoresis in SF performed at 10 hpf. One hour after injection (i.e. at 11 hpf), embryos were photographed to record the dextran injection position on the neural plate (A, bright field, BF; A′, fluorescence, Rhod; A″, merge). Seventeen hours after injection (i.e. at 27 hpf) the eyes and brain were photographed. Several examples are shown (B-E), with labelled cells in the ventral quadrant (vq), the dorsal retina (dr), or both. In all panels, an arrowhead indicates the ventral fissure of the retina, taken as a landmark for the definition of the vq. (**F**,**G**) Fate-map of the anterior neural plate in SF. Injection points are colour-coded according to the location of their progeny. Green, contribution to dorsal retina (dr, ±other forebrain parts); pink, contribution to ventral quadrant (vq, ±other forebrain parts); black, vq+dr; blue, retina (R) + hypothalamus (hyp). The superimposed dotted shading indicates for correlation the typical *Lhx2* expression pattern difference between SF and CF. (**H-J″**) Examples of rhodamine dextran iontophoresis in CF (H-J, bright field; H′-J′, fluorescence; H″-J″, merge). The embryo shown in H-H″ just after injection is also shown in I-I″ at 27 hpf. It contains many cells in the depth of the dorsal retina (dr) and also in the hypothalamus (hyp). (**K**) Fate-map of the anterior neural plate in CF. Colour codes are the same as for SF. Light blue: contribution to the hypothalamus (hyp) ±telencephalon. (**L-N**) CF embryos treated with 2 µM SU5402 between 8 and 12 hpf have a restored ventral quadrant (L,M) comparable with a SF (N). (**O**) Quantification of the effect indicates a ~50% increase of the vq contribution to eye size in treated embryos versus controls. Out of the 16 SU-treated CF embryos, seven showed a normal vq (complete rescue like in 5M), four showed a small vq (partial rescue) and five were not rescued. Conversely, a small but significant decrease in the size of the lens was found. ***P<0.001. Data are mean±s.e.m.

that anterior neural progenitors in CF receive high doses of proliferative signals and/or that a larger progenitor pool may be formed at this rostral level. As preliminary evidence in favour of this possibility, we have found a 33% increase in the number of proliferating cells in the olfactory bulbs of CF at 36 hpf after phospho-histone H3 staining, and we have observed that the CF adult telencephalon is larger anteriorly with bigger olfactory bulbs when compared with SF (see Fig. S4 in the supplementary material). Increasing these two major signalling pathways in CF therefore has pleiotropic outcomes on its forebrain morphogenesis (see also Menuet et al., 2007) (Fig. 6).

The *Fgf8* heterochrony in CF modulates anterior neural plate patterning and impacts eye morphogenesis

Anterior neural plate and eyefield patterning was analysed with two LIM-homeodomain factors, Lhx2 and its paralogue Lhx9, as read-outs of the influence of Shh and Fgf signalling. We choose these markers because they are crucial eye-specification genes. *Lhx2* in particular is required for eye formation (Porter et al., 1997; Tetreault et al., 2009; Yun et al., 2009), and is a member of a small gene network able to induce ectopic eyes (Zuber et al., 2003). We also found strong expression of *Lhx9* in the *Astyanax* 10 hpf neural plate, consistent with recently reported expression of this factor in the *Xenopus* eyefield (Atkinson-Leadbeater et al., 2009). Interestingly, *Lhx2* and *Lhx9* expression patterns differed between CF and SF at the level of the medial neural plate, precisely in spatial relationship with the zone of influence of midline signalling systems. *Lhx2/Lhx9* transcripts thus behave similarly to *Pax6* transcripts in CF (Strickler et al., 2001).

Are the differences in *Lhx2/Lhx9* patterns between CF and SF due to the heterochrony of *Fgf8* or to the heterotopy of *Shh*? The elements to consider when answering this question are as follows. (1) The expression difference in CF versus SF occurs much earlier for *Shh* than for *Fgf8*, suggesting that *Shh* expansion – itself probably driven by earlier events – is at the origin of the Fgf8 signalling modifications in CF. Cyclopamine treatments on CF support this hypothesis. (2) Inhibition of Shh signalling abolishes *Fgf8* expression, and inhibition of Fgf signalling rescues *Lhx2/9* expression in the neural plate but also downregulates *Shh* expression in the hypothalamus, suggesting reciprocal interaction between *Shh* and *Fgf*, and epistatic relationships between Fgf and

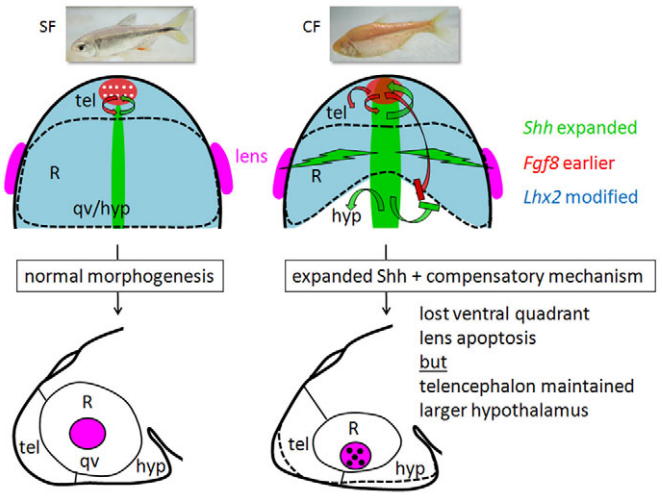

Fig. 6. Signalling and cell fate in the anterior plate in SF and CF embryos and their morphogenetic consequences. None of the regulatory interactions reported on this scheme were shown to be direct. In SF (left), normal expression of Shh (green) and Fgf8 (red with dots) in time and space is followed by 'correct' anterior neural plate patterning, as seen through Lhx2 (blue) expression and correct morphogenesis, in particular of a normal and complete eye with a retina (R), including a vq. In CF (right), expanded Shh has previously been shown to indirectly affect the lens (pink) and induce its apoptosis (black dots) (Yamamoto et al., 2004). Here, we show that increased Shh signalling leads to earlier expression of *Fgf8* (red without dots), a change that is probably responsible for the maintenance of a correct anterior forebrain (tel, telencephalon, horse-shoe shaped). However, it also leads to modifications of patterning and cell fate in the medial part of the neural plate, as deduced from *Lhx2* pattern and fate-mapping experiments that indicate a trade-off between ventral retina (vq) and hypothalamus (hyp) territories. These effects are consistent with our previous findings that the presumptive hypothalamus is enlarged in CF (Menuet et al., 2007; Rétaux et al., 2008) and with preliminary results indicating that the rostral-most telencephalon (olfactory bulbs) are more developed in CF (see Fig. S4 in the supplementary material).

Lhx genes between ~10 and 12 hpf. (3) Recent data showed that although Fgf8 was thought to act downstream of Shh signalling, ectopic Fgf8 downregulates *Lhx2* telencephalic expression in *Shh*-null mice, suggesting that Fgf signalling acts independently of Shh (Okada et al., 2008). In zebrafish, SU5402 treatments have shown that Fgf8 is required for the initiation and maintenance of *Lhx2* expression, whereas using Shh pathway mutants has little effect on *Lhx2* expression (Seth et al., 2006). In *Xenopus*, Fgf signalling is necessary to initiate (but not to maintain) normal expression levels of *x-Lhx9* (Atkinson-Leadbeater et al., 2009). Altogether, these elements suggest that in *Astyanax*, although expanded *Shh* domain is the primary difference observed in CF, it is the *Fgf8* heterochrony that modifies *Lhx2/Lhx9* expression in the medial neural plate. Whether Fgf8 acts directly or not on *Lhx* transcription is an important issue that remains to be determined.

We also bring experimental evidence in favour of the *Shh* expansion and the *Fgf8* heterochrony being (indirectly, through Lhx genes and modulation of the neural plate fate map) responsible for the loss of vq in the CF retina. The SU5402 treatments restoring both a *Lhx2* pattern and a retina morphology mimicking a SF, coupled to the fate-mapping experiments demonstrating that posterior and medial cells of the anterior neural plate contribute to the vq in SF, strongly support this idea. In addition, fully consistent is the fact that the posterior medial cells of the anterior neural plate in CF contribute to the hypothalamus. In addition, a few cells injected in this area were later found in the telencephalon, a result that was never observed in SF. This suggests a 'trade-off' of prospective territories between vq and hypothalamus on the one hand, and between the retina and the telencephalon (as in *Rx3* mutants, see below) on the other hand, in CF embryos. Although the two assays cannot be performed on the same embryos for definitive proof, we propose that the rescue of the vq in SU-treated CF is due to the restoration of a normal, SF-like *Lhx2* expression pattern at neural plate stage.

Whereas regulation in space is often given strong importance, the 'physiological' *Astyanax* CF model further emphasises how regulation in time is also crucial. Of note, the modalities of reciprocal signalling between cells expressing *Shh* and their neighbours expressing *Fgf8* are normal in CF, as suggested by the double in situ hybridisation showing strictly adjacent expression in both CF and SF. Moreover, at stages earlier than 10 hpf and later than 12 hpf, CF and SF display an identical *Fgf8* pattern (see Fig. S1C-E′ in the supplementary material). It is therefore the 2-hour shift in *Fgf8* telencephalic expression that makes the difference. For the CF embryo, this 2-hour advancement happens to affect the vq negatively, but also importantly counteracts and compensates the *Shh*-expanded expression domain and increased signalling onto the rostral neural tube, allowing the CF to develop a normal telencephalon (Fig. 6).

Why do CF first develop eyes?

The fact that CF embryos first develop eyes has puzzled researchers because it appears like a useless dispense of energy. However, from an early neurodevelopmental point of view, it may have been expected. Previous fate-mapping of the zebrafish neural plate (England et al., 2006; Varga et al., 1999; Woo and Fraser, 1995) and the present iontophoresis experiments in *Astyanax* show that cells contributing to the retina and to the rest of the secondary prosencephalon (hypothalamus plus telencephalon) are fairly intermingled at early stages, rendering virtually impossible to develop a normal forebrain without contributing at the same time to the making of an eye. Thus, for a vertebrate embryo, it is probably a strong developmental constraint to make eyes in order to shape a correct forebrain. To our knowledge, there is no case of a viable vertebrate embryo that would never develop eyes. In this line, it is remarkable that 'eye genes' such as *Pax6* or *Lhx2* are also expressed in other parts of the presumptive prosencephalon at late gastrula/early neurula stages and strongly affect telencephalic development in addition to leading to eyeless phenotypes when they are mutated (Bulchand et al., 2001; Mangale et al., 2008; Monuki et al., 2001; Porter et al., 1997; Stoykova et al., 2000). *Rx3* is the only factor reported to segregate very early on the telencephalic and eyefield territories in zebrafish (Stigloher et al., 2006). However, the *Rx3* mutation, which leads to an enlarged telencephalon and a lack of retina, also has deleterious effects on the anterior hypothalamus, which is reduced or missing (Stigloher et al., 2006).

Conclusion

Using CF as an advantageous model, we show that tight temporal regulation of signalling systems during early embryogenesis has a crucial impact on the size and shape of a structure – the vq of the retina. We were able, through manipulation of Fgf signalling, to

restore this vq, which constitutes the neural plate-derived component of the CF eye defect. It is highly probable that the signalling modifications we describe here for Fgf8 will also impact the other, placode-derived component of the eye, the lens, as Shh does (Yamamoto and Jeffery, 2000; Yamamoto et al., 2004). Our results are in favour of the idea that several morphological traits have evolved in cavefish after modification of factors with pleiotropic effects (Menuet et al., 2007; Protas et al., 2006; Yamamoto et al., 2009). They also highlight the power of developmental heterochronies in the evolution of morphological characters.

Acknowledgements
Work supported by ANR-Neuro (Agence Nationale pour la Recherche) [Midline] and CNRS (Centre National de la Recherche Scientifique) to S.R. K.P. was supported by a PhD fellowship from the French Ministry of Research and by Agence pour la Recherche sur le Cancer. We thank Stéphane Père for taking care of our *Astyanax* colony, Mickael Poidevin for assistance with qPCR, Aurélie Heuzé for technical support, Nadine Peyrieras for help and access to iontophoresis set-up, and an anonymous referee for his/her very insightful remarks.

Competing interests statement
The authors declare no competing financial interests.

Supplementary material
Supplementary material for this article is available at
http://dev.biologists.org/lookup/suppl/doi:10.1242/dev.054106/-/DC1

References
Alunni, A., Menuet, A., Candal, E., Penigault, J. B., Jeffery, W. R. and Rétaux, S. (2007). Developmental mechanisms for retinal degeneration in the blind cavefish Astyanax mexicanus. *J. Comp. Neurol.* **505**, 221-233.
Atkinson-Leadbeater, K., Bertolesi, G. E., Johnston, J. A., Hehr, C. L. and McFarlane, S. (2009). FGF receptor dependent regulation of Lhx9 expression in the developing nervous system. *Dev. Dyn.* **238**, 367-375.
Bulchand, S., Grove, E. A., Porter, F. D. and Tole, S. (2001). LIM-homeodomain gene Lhx2 regulates the formation of the cortical hem. *Mech. Dev.* **100**, 165-175.
Chen, J. K., Taipale, J., Young, K. E., Maiti, T. and Beachy, P. A. (2002). Small molecule modulation of Smoothened activity. *Proc. Natl. Acad. Sci. USA* **99**, 14071-14076.
Crossley, P. H., Martinez, S., Ohkubo, Y. and Rubenstein, J. L. (2001). Coordinate expression of Fgf8, Otx2, Bmp4, and Shh in the rostral prosencephalon during development of the telencephalic and optic vesicles. *Neuroscience* **108**, 183-206.
Deyts, C., Candal, E., Joly, J. S. and Bourrat, F. (2005). An automated in situ hybridization screen in the Medaka to identify unknown neural genes. *Dev. Dyn.* **234**, 698-708.
Echelard, Y., Epstein, D. J., St-Jacques, B., Shen, L., Mohler, J., McMahon, J. A. and McMahon, A. P. (1993). Sonic hedgehog, a member of a family of putative signaling molecules, is implicated in the regulation of CNS polarity. *Cell* **75**, 1417-1430.
England, S. J., Blanchard, G. B., Mahadevan, L. and Adams, R. J. (2006). A dynamic fate map of the forebrain shows how vertebrate eyes form and explains two causes of cyclopia. *Development* **133**, 4613-4617.
Fukuchi-Shimogori, T. and Grove, E. A. (2001). Neocortex patterning by the secreted signaling molecule FGF8. *Science* **294**, 1071-1074.
Gibert, Y., Bernard, L., Debiais-Thibaud, M., Bourrat, F., Joly, J. S., Pottin, K., Meyer, A., Rétaux, S., Begemann, G. and Laudet, V. (2010). Formation of oral and pharyngeal dentition in teleosts depends on differential recruitment of retinoic acid signaling. *FASEB J.* **24**, 3298-3309.
Hayhurst, M., Gore, B. B., Tessier-Lavigne, M. and McConnell, S. K. (2008). Ongoing sonic hedgehog signaling is required for dorsal midline formation in the developing forebrain. *Dev. Neurobiol.* **68**, 83-100.
Houart, C., Caneparo, L., Heisenberg, C., Barth, K., Take-Uchi, M. and Wilson, S. (2002). Establishment of the telencephalon during gastrulation by local antagonism of Wnt signaling. *Neuron* **35**, 255-265.
Incardona, J. P., Gaffield, W., Kapur, R. P. and Roelink, H. (1998). The teratogenic Veratrum alkaloid cyclopamine inhibits sonic hedgehog signal transduction. *Development* **125**, 3553-3562.
Jeffery, W. R. (2001). Cavefish as a model system in evolutionary developmental biology. *Dev. Biol.* **231**, 1-12.
Jeffery, W. R. (2005). Adaptive evolution of eye degeneration in the Mexican blind cavefish. *J. Hered.* **96**, 185-196.
Jeffery, W. R. (2008). Emerging model systems in evo-devo: cavefish and microevolution of development. *Evol. Dev.* **10**, 265-272.
Jeffery, W. R. (2009). Regressive evolution in Astyanax cavefish. *Annu. Rev. Genet.* **43**, 25-47.
Lee, K. J. and Jessell, T. M. (1999). The specification of dorsal cell fates in the vertebrate central nervous system. *Annu. Rev. Neurosci.* **22**, 261-294.
Liem, K. F., Jr, Tremml, G. and Jessell, T. M. (1997). A role for the roof plate and its resident TGFbeta-related proteins in neuronal patterning in the dorsal spinal cord. *Cell* **91**, 127-138.
Mangale, V. S., Hirokawa, K. E., Satyaki, P. R., Gokulchandran, N., Chikbire, S., Subramanian, L., Shetty, A. S., Martynoga, B., Paul, J., Mai, M. V. et al. (2008). Lhx2 selector activity specifies cortical identity and suppresses hippocampal organizer fate. *Science* **319**, 304-309.
Menuet, A., Alunni, A., Joly, J. S., Jeffery, W. R. and Rétaux, S. (2007). Expanded expression of Sonic Hedgehog in *Astyanax* cavefish: multiple consequences on forebrain development and evolution. *Development* **134**, 845-855.
Miyake, A., Nakayama, Y., Konishi, M. and Itoh, N. (2005). Fgf19 regulated by Hh signaling is required for zebrafish forebrain development. *Dev. Biol.* **288**, 259-275.
Mohammadi, M., McMahon, G., Sun, L., Tang, C., Hirth, P., Yeh, B. K., Hubbard, S. R. and Schlessinger, J. (1997). Structures of the tyrosine kinase domain of fibroblast growth factor receptor in complex with inhibitors. *Science* **276**, 955-960.
Monuki, E. S. (2007). The morphogen signaling network in forebrain development and holoprosencephaly. *J. Neuropathol. Exp. Neurol.* **66**, 566-575.
Monuki, E. S., Porter, F. D. and Walsh, C. A. (2001). Patterning of the dorsal telencephalon and cerebral cortex by a roof plate-Lhx2 pathway. *Neuron* **32**, 591-604.
Muroyama, Y., Fujihara, M., Ikeya, M., Kondoh, H. and Takada, S. (2002). Wnt signaling plays an essential role in neuronal specification of the dorsal spinal cord. *Genes Dev.* **16**, 548-553.
Ohkubo, Y., Chiang, C. and Rubenstein, J. L. (2002). Coordinate regulation and synergistic actions of BMP4, SHH and FGF8 in the rostral prosencephalon regulate morphogenesis of the telencephalic and optic vesicles. *Neuroscience* **111**, 1-17.
Okada, T., Okumura, Y., Motoyama, J. and Ogawa, M. (2008). FGF8 signaling patterns the telencephalic midline by regulating putative key factors of midline development. *Dev. Biol.* **320**, 92-101.
Porter, F. D., Drago, J., Xu, Y., Cheema, S. S., Wassif, C., Huang, S. P., Lee, E., Grinberg, A., Massalas, J. S., Bodine, D. et al. (1997). Lhx2, a LIM homeobox gene, is required for eye, forebrain, and definitive erythrocyte development. *Development* **124**, 2935-2944.
Protas, M. E., Hersey, C., Kochanek, D., Zhou, Y., Wilkens, H., Jeffery, W. R., Zon, L. I., Borowsky, R. and Tabin, C. J. (2006). Genetic analysis of cavefish reveals molecular convergence in the evolution of albinism. *Nat. Genet.* **38**, 107-111.
Protas, M., Conrad, M., Gross, J. B., Tabin, C. and Borowsky, R. (2007). Regressive evolution in the Mexican cave tetra, Astyanax mexicanus. *Curr. Biol.* **17**, 452-454.
Rétaux, S., Pottin, K. and Alunni, A. (2008). Shh and forebrain evolution in the blind cavefish *Astyanax mexicanus*. *Biol. Cell* **100**, 139-147.
Rose, F. L. and Mitchell. R. W. (1982). Comparative lipid values of epigean and cave-adapted *Astyanax*. *Southwest. Nat.* **27**, 357-358.
Salin, K., Voituron, Y., Mourin, J. and Hervant, F. (2010). Cave colonization without fasting capacities: an example with the fish *Astyanax fasciatus mexicanus*. *Comp. Biochem. Physiol.* **156A**, 451-457.
Seth, A., Culverwell, J., Walkowicz, M., Toro, S., Rick, J. M., Neuhauss, S. C., Varga, Z. M. and Karlstrom, R. O. (2006). belladonna/(lhx2) is required for neural patterning and midline axon guidance in the zebrafish forebrain. *Development* **133**, 725-735.
Shanmugalingam, S., Houart, C., Picker, A., Reifers, F., Macdonald, R., Barth, A., Griffin, K., Brand, M. and Wilson, S. W. (2000). Ace/Fgf8 is required for forebrain commissure formation and patterning of the telencephalon. *Development* **127**, 2549-2561.
Shimamura, K. and Rubenstein, J. L. (1997). Inductive interactions direct early regionalization of the mouse forebrain. *Development* **124**, 2709-2718.
Shimogori, T., Banuchi, V., Ng, H. Y., Strauss, J. B. and Grove, E. A. (2004). Embryonic signaling centers expressing BMP, WNT and FGF proteins interact to pattern the cerebral cortex. *Development* **131**, 5639-5647.
Stigloher, C., Ninkovic, J., Laplante, M., Geling, A., Tannhauser, B., Topp, S., Kikuta, H., Becker, T. S., Houart, C. and Bally-Cuif, L. (2006). Segregation of telencephalic and eye-field identities inside the zebrafish forebrain territory is controlled by Rx3. *Development* **133**, 2925-2935.
Storm, E. E., Garel, S., Borello, U., Hebert, J. M., Martinez, S., McConnell, S. K., Martin, G. R. and Rubenstein, J. L. (2006). Dose-dependent functions of Fgf8 in regulating telencephalic patterning centers. *Development* **133**, 1831-1844.

Stoykova, A., Treichel, D., Hallonet, M. and Gruss, P. (2000). Pax6 modulates the dorsoventral patterning of the mammalian telencephalon. *J. Neurosci.* **20**, 8042-8050.
Strickler, A. G., Yamamoto, Y. and Jeffery, W. R. (2001). Early and late changes in Pax6 expression accompany eye degeneration during cavefish development. *Dev. Genes Evol.* **211**, 138-144.
Strickler, A. G., Yamamoto, Y. and Jeffery, W. R. (2007). The lens controls cell survival in the retina: Evidence from the blind cavefish Astyanax. *Dev. Biol.* **311**, 512-523.
Tetreault, N., Champagne, M. P. and Bernier, G. (2009). The LIM homeobox transcription factor Lhx2 is required to specify the retina field and synergistically cooperates with Pax6 for Six6 trans-activation. *Dev. Biol.* **327**, 541-550.
Toro, S. and Varga, Z. M. (2007). Equivalent progenitor cells in the zebrafish anterior preplacodal field give rise to adenohypophysis, lens, and olfactory placodes. *Semin. Cell Dev. Biol.* **18**, 534-542.
Varatharasan, N., Croll, R. P. and Franz-Odendaal, T. (2009). Taste bud development and patterning in sighted and blind morphs of Astyanax mexicanus. *Dev. Dyn.* **238**, 3056-3064.
Varga, Z. M., Wegner, J. and Westerfield, M. (1999). Anterior movement of ventral diencephalic precursors separates the primordial eye field in the neural plate and requires cyclops. *Development* **126**, 5533-5346.
Vieira, C., Pombero, A., Garcia-Lopez, R., Gimeno, L., Echevarria, D. and Martinez, S. (2010). Molecular mechanisms controlling brain development: an overview of neuroepithelial secondary organizers. *Int. J. Dev. Biol.* **54**, 7-20.
Walshe, J. and Mason, I. (2003). Unique and combinatorial functions of Fgf3 and Fgf8 during zebrafish forebrain development. *Development* **130**, 4337-4349.
Westerfield, M. (2000). *The Zebrafish Book. A Guide for the Laboratory Use of Zebrafish (Danio rerio)*. Eugene, OR: University of Oregon Press.
Wilkens, H. (2007). Regressive evolution: ontogeny and genetics of cavefish eye rudimentation. *Biol. J. Linn. Soc.* **92**, 287-296.
Woo, K. and Fraser, S. E. (1995). Order and coherence in the fate map of the zebrafish nervous system. *Development* **121**, 2595-2609.
Yamamoto, Y. and Jeffery, W. R. (2000). Central role for the lens in cave fish eye degeneration. *Science* **289**, 631-633.
Yamamoto, Y. and Jeffery, W. R. (2002). Probing teleost eye development by lens transplantation. *Methods* **28**, 420-426.
Yamamoto, Y., Stock, D. W. and Jeffery, W. R. (2004). Hedgehog signalling controls eye degeneration in blind cavefish. *Nature* **431**, 844-847.
Yamamoto, Y., Byerly, M. S., Jackman, W. R. and Jeffery, W. R. (2009). Pleiotropic functions of embryonic sonic hedgehog expression link jaw and taste bud amplification with eye loss during cavefish evolution. *Dev. Biol.* **330**, 200-211.
Young, N. M., Chong, H. J., Hu, D., Hallgrímsson, B. and Marcucio, R. S. (2010). Quantitative analyses link modulation of sonic hedgehog signaling to continuous variation in facial growth and shape. *Development* **137**, 3405-3409.
Yun, S., Saijoh, Y., Hirokawa, K. E., Kopinke, D., Murtaugh, L. C., Monuki, E. S. and Levine, E. M. (2009). Lhx2 links the intrinsic and extrinsic factors that control optic cup formation. *Development* **136**, 3895-3906.
Zhoua, X. and Vize, P. D. (2004). Proximo-distal specialization of epithelial transport processes within the *Xenopus* pronephric kidney tubules. *Dev. Biol.* **271**, 322-338.
Zuber, M. E., Gestri, G., Viczian, A. S., Barsacchi, G. and Harris, W. A. (2003). Specification of the vertebrate eye by a network of eye field transcription factors. *Development* **130**, 5155-5167.